

# MEMS-enabled Reconfigurable VCO and RF Filter

Deepa Ramachandran<sup>\*</sup>, Altug Oz<sup>\*</sup>, Vivek Kumar Saraf<sup>\*</sup>, Gary K. Fedder<sup>\*†</sup> and Tamal Mukherjee<sup>\*</sup>

<sup>\*</sup>Department of Electrical and Computer Engineering and <sup>†</sup>The Robotics Institute, Carnegie Mellon University, 5000 Forbes Ave., Pittsburgh, PA 15213-3890, USA.

**Abstract** — RF building block circuits that can reconfigure from one frequency to another are of interest in multifunction radios. Reconfigurable MEMS capacitors are integrated with on-chip inductors and transistors to design reconfigurable VCO and filter circuits. Electrothermal actuation of the MEMS capacitor leads to >400 MHz change in operating frequency.

**Index Terms** — Frequency hop communication, filter, voltage controlled oscillators, micromachining, inductor, varactor.

## I. INTRODUCTION

Recent interest in reconfigurable radio has focused on software reconfiguration, with an ADC at the front end directly transforming the radio signal into digital bits. As high-speed, high-resolution ADCs invariably require high power consumption, hardware reconfigurable front ends that can synergistically integrate with software radios are required. An approach to hardware reconfiguration for RF systems is a reconfigurable capacitor [1] that can dynamically change between two capacitance values.

Micromachined capacitors have previously been connected to off-chip inductors and electronics using bondwires for VCO [2] and RF filter applications [3]. Compared with solid-state varactors, MEMS tunable capacitors have advantages of lower loss, larger tuning range and more linear tuning characteristics. Prior work in MEMS capacitors have used customized processing, preventing integration with on-chip inductors or solid-state devices. This paper implements a CMOS-compatible reconfigurable capacitor [1] in a foundry SiGe BiCMOS process incorporating high performance active devices and RF passives. A VCO and RF filter design using these elements is used to demonstrate the potential of MEMS capacitors to achieve wide tuning range without trading off other performance goals.

## II. INTEGRATED RECONFIGURABLE MEMS CAPACITOR

The capacitor is formed by interdigitated beams fabricated using interconnect layers in the BiCMOS process. Micromachining [4] the chip after foundry fabrication allows sets of beams to move with respect to each other. The capacitance is changed by moving one set of beams with respect to the other, thereby changing the gap between

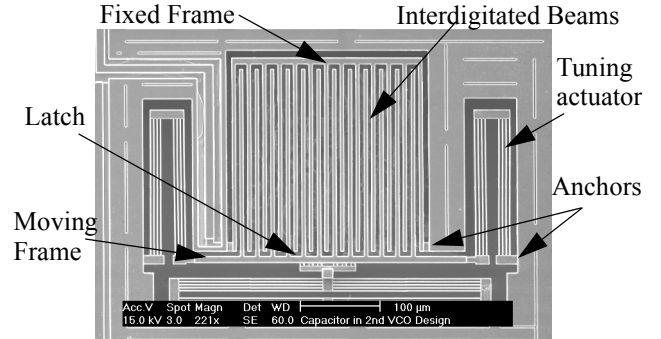


Fig. 1. Interdigitated beam MEMS reconfigurable capacitor.

the beams. The capacitor operation is illustrated in Fig. 1. When the capacitors are released by the micromachining process, the beams mounted on the moveable frame move to the right (away from the beams attached to the fixed frame) due to a designed-in lateral stress gradient in the tuning actuators. This self-assembly process leaves the capacitance in its *disengaged* (or  $C_{\min}$ ) state.

Driving current through the embedded polysilicon resistors in the tuning actuator leads to electrothermal actuation due to differences in the temperature coefficient of expansion (TCE) of the layers used in the actuator beams. This lateral electrothermal actuation moves the inner frame to the *engaged* (or  $C_{\max}$ ) state. For large tuning range (> 200 %), the engaged gap is minimized (< 0.3  $\mu\text{m}$ ), and the disengaged gap is maximized (> 2.5  $\mu\text{m}$ ) [5].

For operation with zero-standby power, a lateral latch composed of a “peg” in a slot is used. Two slots are needed: one for the disengaged position, and the other for the engaged position. After release, the self-assembly motion leads to the peg being trapped in the disengaged slot. The device is then moved to the engaged slot through a sequence of heating and cooling operations on the tuning and latch actuators. Multiple slots can be used to obtain multiple capacitance values from the same capacitor.

## III. FREQUENCY-HOPPING CIRCUITS WITH RF MEMS RECONFIGURABLE CAPACITOR

VCO and filter circuits were designed that exploit the reconfigurable capacitor for frequency hopping. For this paper we focus only on dual-frequency operation. Hence only two latch slots are needed in the capacitor.

### A. LC-based VCO

Reconfigurable capacitors can be exploited in a Voltage Controlled Oscillator (VCO) to provide digital reconfiguration in addition to the analog tuning from MOS varactor or varactor diodes. The advantage of this scheme is additional tuning range without increasing the size of the lossy, non-linear foundry-provided varactor diode. Linearization can be achieved by connecting a fixed capacitor in series [6] or parallel [7] with the varactor. The former is at the expense of tuning range while the latter requires additional mixed-signal control. In the reconfigurable capacitor, a zero-power micromechanical latch is used for gap control. Also, wider tuning range is achieved because of lower parasitics in the micromachined capacitor.

Among the standard cross-coupled topologies used for VCO's, namely, nMOS, CMOS and bipolar, the bipolar implementation was selected as it allows more voltage swing compared to CMOS and a higher  $g_m/I$  ratio compared to nMOS. The high voltage swing is achieved by decoupling the base and collector of the cross coupled pair with a capacitive divider as shown in Fig 2, preventing forward bias of the C-B junction. The large voltage swing in turn leads to better phase noise in accordance with the classical Leeson's model [8],

$$PN(f_m) = \frac{2 \cdot k \cdot T \cdot F \cdot R_p}{A_o^2} \left( \frac{f_o}{2 \cdot Q \cdot f_m} \right)^2 \left( 1 + \frac{\Delta f_{1/f^3}}{f_m} \right)^2 \quad (1)$$

where  $k$  is Boltzmann's constant,  $T$  is the absolute temperature,  $A_o$  is the amplitude of oscillation,  $Q$  is the resonator loaded quality factor,  $R_p$  is the parallel resistance used to model the losses in the resonator,  $\Delta f_{1/f^3}$  is the  $1/f^3$  corner frequency in the phase noise spectrum and  $F$  is the excess noise factor. Hence it can be seen that the phase noise

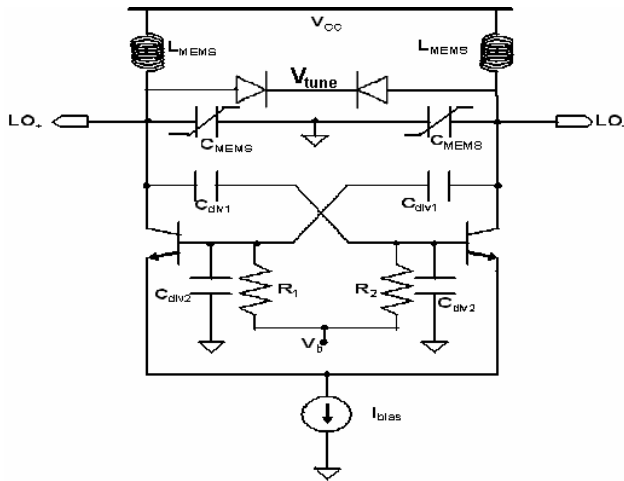


Fig. 2. VCO Schematic

drops as the square of the oscillation amplitude. The LC tank consists of the micromachined high-Q 6.25 nH inductor [9], a MEMS reconfigurable capacitor for digital tuning between 1.8 and 3.1 GHz and a foundry-provided varactor diode for analog tuning of 150 MHz around these two set points.

### B. LC-based Filter

Reconfigurable capacitors are combined with an inductor as a  $\pi$ -network filter (Fig 3) to switch between two desired center frequencies with high Q and low insertion loss. A secondary goal is to achieve similar insertion loss at both operating frequencies.

The center frequency of the filter can be approximated as  $\omega_0 = \sqrt{1/(L(C_{tank} + C_{dc}))}$ , with the components labelled in Fig 3. Assuming lossless passives, the Q factor is

$$Q = \frac{2}{\omega_0 R_l} \left( \frac{C_{tank} + C_{dc}}{C_{dc}^2} \right) + 2\omega_0 R_l C_{tank} \quad (2)$$

where  $R_l$  is the load resistance and  $\omega_0$  is the center frequency. High filter Q requires a high  $C_{tank}/C_{dc}$  ratio.

Integrated RF filters have poor insertion loss due to the low inductor Q [10]. In this design, insertion loss is minimized with a high-Q inductor [9]. For the  $\pi$ -network, with a lossy tank, insertion loss can also be minimized with a low  $C_{tank}/C_{dc}$  ratio. During design, different  $C_{tank}/C_{dc}$  ratios were chosen to compensate for difference in inductor Q, and to account for interconnect parasitic capacitances at the two frequencies. Optimizing Q and insertion loss requires moving the  $C_{tank}/C_{dc}$  ratio in different directions. This trade-off in Q and insertion loss is a limitation of this topology.

The design process began by targeting two center frequencies: 1.7 and 2.6 GHz as that covers a wide range of low cost portable communications frequencies. First, an inductor value was chosen while considering that smaller inductors allows larger capacitors that can have larger  $\Delta C$ , thereby increasing tuning range. Secondly, the  $C_{tank}/C_{dc}$  ratio was chosen for a filter Q greater than 5 and insertion loss less than 5 dB. Other design limitations such as on-chip realizable dimensions of the RF passives and parasitic interconnect capacitance (for wiring the inductor to MEMS capacitors and the MEMS capacitors to pads) were also

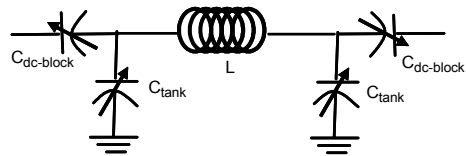


Fig. 3. RF frequency hopping filter schematic.

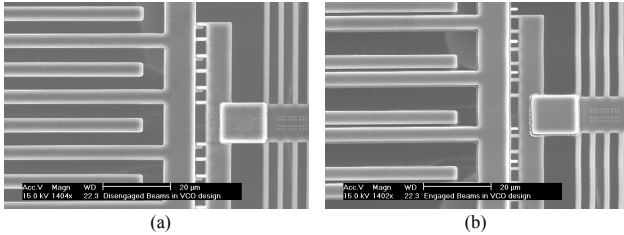


Fig. 4. Scanning electron micrograph (SEM) of a fabricated capacitor. (a) capacitor in disengaged ( $C_{\min}$ ) state, (b) capacitor in engaged ( $C_{\max}$ ) state.

considered. Circuit simulation using a modified lumped parameter model of the inductor (to include micromachining effects) and the capacitor showed insertion loss of -4.7 and -5 dB, respectively, and Q values of 5.3 and 7.1, respectively.

#### IV. MEASUREMENT RESULTS

The circuits were fabricated in a Jazz 0.35  $\mu\text{m}$  BiCMOS process. The chips were post-processed using a sequence of steps similar to [4] to release the MEMS varactor. The chips were tested using the Agilent E8364A Network Analyzer and Cascade Microtech 6" RF probe station with ACP GSG probes.

##### A. RF MEMS Reconfigurable Capacitor

A test capacitor was included on the chip for device characterization. The latch mechanism sets the gap as designed for the disengaged state. Polymer formation on the beam sidewalls prevented achieving the designed gap at the engaged state. The observed self-assembly and electrothermal actuation directions are the same as predicted. The SEMs in Fig 4(a) and Fig 4(b) show the disengaged and engaged states, respectively. To release the latch from

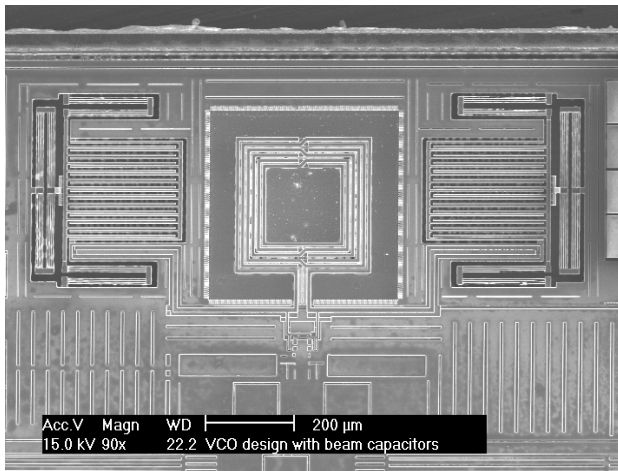


Fig. 5. SEM of VCO with two reconfigurable capacitances and a center-tapped differential inductor at the top, and the core circuit at the bottom.

TABLE 1.  
VCO PERFORMANCE

	$f_o$ (GHz)	PN @ 1MHz (dBc/Hz)	$P_{\text{diss}}$ (mW)	Tuning Range (%)
$C_{\min}$ config.	2.8	-122	3.5	30
$C_{\max}$ config.	2.1	-122	5	30
[6]	1.8	-130	20	16
[7]	1.7	-122	24	26

the disengaged state, a dc 4.5 V control signal was used to heat the electrothermal latch actuators. In the design 4 V dc control signal was supposed to move the tuning actuators to the engaged state. In the reported measurements, a 0 V dc control voltage was used to achieve the  $C_{\max}$  configuration. The measured gap at  $C_{\min}$  was 2.8  $\mu\text{m}$  and at  $C_{\max}$  was 0.3  $\mu\text{m}$ , and the measured capacitance values were 400 fF and 866 fF, respectively. The resulting tuning range is 217%. The measured quality factor exceeds 30 for the frequency ranges of the filter and VCO circuits.

##### B. RF Frequency-Hopping VCO

The SEM of the VCO is shown in Fig 5. The carrier frequencies obtained as a result of the digital tuning are 2.75 GHz ( $C_{\min}$  configuration) and 2.15 GHz ( $C_{\max}$  configuration). Along with analog tuning, the minimum and maximum frequencies obtained are 2.1 GHz and 2.8 GHz respectively, resulting in a tuning range of 30 % for a center frequency of 2.45 GHz. Table 1, shows not only the superior tuning range of this design but also highlights its low power consumption compared to previously published designs. To maintain the same carrier power (-4 dBm) and phase noise (-122 dBc/Hz @ 1MHz), current consumption is higher for the  $C_{\max}$  configuration, because of the increased tank capacitance. The phase noise spectrum at 2.2 GHz is shown in Fig 6.

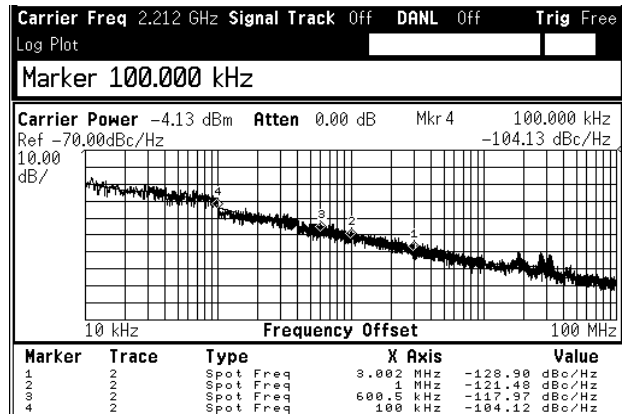


Fig. 6. Oscillator Phase Noise

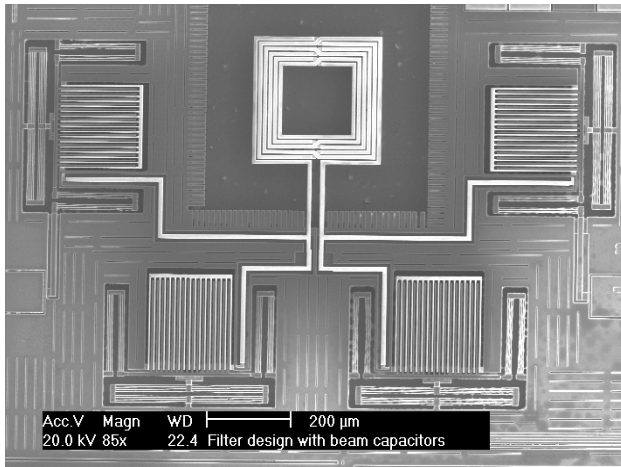


Fig. 7. SEM of filter with inductor (differential layout) and 4 reconfigurable capacitors (tank capacitors are at bottom).

### C. RF Frequency-Hopping Filter

Fig 7 shows the SEM of the released filter. Fig 8 shows the measured  $S_{21}$  response of the filter at the minimum and maximum center frequencies observed. The filter operated at 1.87 GHz (engaged state) to 2.36 GHz (disengaged state). The change in center frequencies achieved is 490 MHz, showing a 23% tuning range at 2.1 GHz. The insertion loss values are -14.3 dB and -19.3 dB, respectively. The quality factor values are 4.4 and 9.5, respectively. Due to incomplete release of one of the tank capacitors ( $C_{tank}$ ), the measured tuning range was lower than the designed tuning range. The larger capacitance of the unreleased capacitor lowered the  $C_{tank}/C_{dc}$  ratio, leading to the increased insertion loss seen in the measurements.

## V. CONCLUSION

Reconfigurable MEMS capacitors are integrated with a high-Q MEMS inductor to form a passive reconfigurable filter. A VCO integrating the MEMS capacitor and induc-

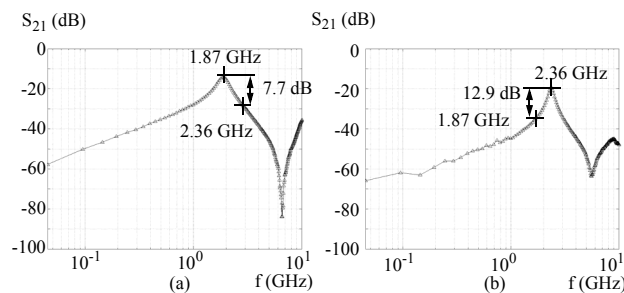


Fig. 8. Measured  $S_{21}$  response for RF frequency-hopping filter at (a) minimum frequency, (b) maximum frequency, showing a frequency hop of 490 MHz. The filter rejects at least 7.7 dB of the undesirable frequency component.

tor with SiGe transistors and varactor diodes was also designed. These circuits showed the ability to switch between frequencies that are more than 400 MHz apart using a reconfigurable capacitor with about 200% tuning range. Detailed characterization of the mechanical material properties of the thin films forming the actuators in the MEMS capacitor combined with improved processing to ensure capacitor release are under way. We expect to be able to achieve capacitor tuning ranges beyond 300%, leading to wideband hopping circuits.

## ACKNOWLEDGEMENT

This research effort was supported by the MARCO/DARPA Focus Center on Circuits and Systems Solutions (C2S2) under award MDA972-02-1-0004 and by DARPA NMASP program under award DAAB07-02-C-K001 and DARPA NeoCAD program under award F33615-01-2-1970.

## REFERENCES

- [1] A. Oz, G. K. Fedder, "CMOS-Compatible RF-MEMS Tunable Capacitors," *2003 IEEE MTT-S Int. RFIC Symp.*, pp. 611-614.
- [2] A. Dec, K. Suyama, "A 1.9-GHz CMOS VCO with micro-machined electromechanically tunable capacitors," *IEEE JSSC*, SC-35(8), August 2000, pp. 1231-1237.
- [3] R.L. Borwick III, P.A. Stupar, J. DeNatale, R. Anderson, R. Erladson, "Variable MEMS capacitors implemented into RF filter systems," *IEEE Trans. Microwave Theory and Techniques*, vol. 51, no. 1, pp. 315-319, Jan. 2003.
- [4] G. K. Fedder, S. Santhanam, M. L. Reed, S. C. Eagle, D. F. Guillou, M. S.-C. Lu, and L. R. Carley, "Laminated High-Aspect-Ratio Microstructures In A Conventional CMOS Process," *Sensors & Actuators*, pp. 103-110, March 1997.
- [5] A. Oz, G.K. Fedder, "CMOS/BiCMOS Self-assembling and electrothermal microactuators for tunable capacitors, nanometer-scale gap-closing structures and latch mechanisms," *Tech. Dig. of the Solid-State Sensor, Actuator and Microsystems Workshop*, June 6-10, 2004, Hilton Head, SC.
- [6] M. Tiebout, "Low-power low-phase-noise differentially tuned quadrature VCO design in standard CMOS," *IEEE JSSC*, SC-36(7), pp. 1018-1024, July 2001.
- [7] A. Kral, F. Behbahani, and A.A. Abidi, "RF-CMOS oscillators with switched tuning," in *Proc. IEEE Custom Integrated Circuits Conf.*, Santa Clara, CA, 1998, pp. 555-558.
- [8] D. B. Leeson, "A Simple Model of Feedback Oscillator Noise Spectrum," *Proc. IEEE*, 54(2), pp. 329-330, 1996.
- [9] H. Lakdawala, X. Zhu, H. Luo, S. Santhanam, L. R. Carley, G. K. Fedder, "Micromachined High-Q Inductors in 0.18  $\mu\text{m}$  Cu Interconnect Low-K CMOS," *IEEE JSSC*, SC-37(3), Mar. 2002, pp. 394-403.
- [10] T. Soorapanth, S.S. Wong, "A 0-dB IL 2140 $\pm$ 30 MHz band-pass filter utilizing Q-enhanced spiral inductors in standard CMOS," *IEEE JSSC*, SC-37(5), pp. 579-586, May 2002.